

Programmed death ligand 1 gene silencing in murine glioma models reveals cell line-specific modulation of tumor growth in vivo

Evelina Blomberg, Manuela Silginer, Patrick Roth, and Michael Weller[®]

Laboratory of Molecular Neuro-Oncology, Department of Neurology, University of Zürich, Zurich, Switzerland (E.B., P.R., M.W.); Department of Neurology, University Hospital Zurich, Zurich, Switzerland (M.S., P.R., M.W.)

Corresponding Author: Michael Weller, Department of Neurology, University Hospital Zurich, Frauenklinikstrasse 26, 8091 Zurich, Switzerland (Michael.Weller@usz.ch).

Abstract

Background. Glioblastoma is the most common brain tumor in adults and virtually incurable. Therefore, new therapeutic strategies are urgently needed. Immune checkpoint inhibition has not shown activity in various phase III trials and intra- as well as intertumoral expression of programmed death ligand 1 (PD-L1) varies in glioblastoma.

Methods. We abrogated constitutive PD-L1 gene expression by CRISPR/Cas9 in murine glioma models and characterized the consequences of gene deletion in vitro and in vivo.

Results. A heterogeneous expression of *Pdl1* mRNA and PD-L1 protein was detected in the glioma cell panel in vitro and in vivo. PD-L1, but not PD-L2, was inducible by interferon β and γ . Co-culture with splenocytes induced PD-L1 expression in GL-261 and SMA-560, but not in CT-2A cells, in an interferon γ -dependent manner. Conversely, *Pdl1* gene silencing conferred a survival benefit in CT-2A, but not in the other 2 models. Accordingly, PD-L1 antibody prolonged survival in CT-2A glioma-bearing mice. This activity required PD-L1 expression on tumor rather than host cells, and the survival gain mediated by PD-L1 loss was reproduced in immune-deficient RAG^{-/-} mice.

Conclusions. PD-L1 is expressed and interferon-inducible in murine glioma cell lines. PD-L1 has model-specific roles for tumor growth. Future studies need to determine which subset of glioblastoma patients may benefit from PD-L1 antagonism as part of a multimodality therapeutic approach to glioblastoma.

Key Points

- Mouse glioma cells express PD-L1 in vitro and in vivo.
- *Pdl1* gene silencing affects tumor growth in vivo in a cell line-specific manner.
- The efficacy of PD-L1 antagonism in the CT-2A model requires PD-L1 expression on tumor cells.

There is an urgent need for novel therapies for glioblastoma. Much effort has been invested into trying to develop more active treatments, but so far, first-line treatment remains to consist of surgery, radiotherapy, and concomitant and maintenance chemotherapy with temozolomide (TMZ).¹ Overall survival remains in the range of 1 year on a population level.^{1–3} Immunotherapy has emerged as a promising new therapeutic area to explore within the field of oncology, including malignant brain tumors.⁴

Immune checkpoints are endogenous negative immune regulatory pathways that function to limit immune responses, to maintain self-tolerance, and to thereby prevent autoimmunity. T cells express a set of inhibitory receptors: when the corresponding ligand bind to these receptors, a negative signaling cascade is triggered.^{5,6}

Tumors may hijack this function by upregulating immune checkpoint ligands on their cell surface. When activated T cells

Importance of the Study

Immune checkpoint inhibition has dramatically changed the therapeutic armamentarium for patients with many solid cancers, but not yet primary brain tumors, including glioblastoma. To what extent programmed death ligand 1 (PD-L1) mediates the immunosuppression in glioblastoma remains controversial. The present study illustrates that PD-L1 gene disruption

affects the tumor growth of commonly used mouse glioma models in a cell line-specific manner. Specifically, in the CT-2A model, the therapeutic activity of PD-L1 antagonism acted on PD-L1 expressed on the tumor rather than host cells. Altogether, these studies further refine the current knowledge on the PD-1/PD-L1 system in glioblastoma.

bind immune checkpoint ligands expressed on tumor cells, their function is impaired and tumor cells evade immune surveillance.^{7,8} Pharmacological intervention using blocking antibodies to the immune checkpoint molecules cytotoxic T-lymphocyte-associated protein 4 (CTLA-4) or programmed cell death protein 1 (PD-1), or to the ligand of PD-1 (PD-L1), have transformed the therapeutic options for several solid cancers, notably those characterized by high tumor mutational burden.^{9–11}

Expression of PD-L1 is not restricted to tumor cells. Multiple cell types of the tumor microenvironment may express PD-L1, most notably tumor-associated macrophages (TAM). Since these cells make up a substantial amount of the tumor core in glioblastoma, they may provide a major contribution to immunosuppression in glioblastoma.¹² Immunohistochemistry indicated that PD-L1 protein is present to a higher extent in glioma tissue than in normal brain.¹³ PD-L1 quantification remains challenging since high variation among different antibody clones has been observed.¹⁴ Data on the prognostic value of PD-L1 mRNA or protein levels therefore remain inconclusive, although several studies have suggested that elevated PD-L1 mRNA¹⁵ or protein levels^{16–18} are associated with shorter overall survival in glioma patients. In contrast, TCGA-based analyses and other studies did not find such a relationship between PD-L1 expression and overall survival in glioblastoma.^{19–21}

In addition to the immune modulatory activity, backward signaling of PD-L1 independent of PD-1, mediating increase in proliferation in vitro and in vivo as well as promoting epithelial mesenchymal transition has been reported in ovarian and esophageal cancer cells, respectively.^{22,23} Accordingly, in the present study, we explored the consequences of PD-L1 gene disruption in murine glioma models in vitro and in vivo.

supplemented with 10% fetal calf serum (FCS) and 2 mM L-glutamine (Gibco Life Technologies, Zug, Switzerland).

Reagents

Murine interferon (IFN)- β 1a was kindly provided by Biogen (Cambridge, MA). Recombinant murine IFN- γ was obtained from PeproTech (Rocky Hill, NJ). Anti-PD-L1 (clone 6E11) was kindly provided by Genentech (South San Francisco, CA).

CRISPR Genome Editing

Two single guide RNA (sgRNA) sequences targeting *Pd-1* were generated by using the MIT Optimized CRISPR Design Tool (<http://crispr.mit.edu/>). All sgRNA sequences had high scores (>88) to minimize off-target effects. The following sgRNA sequences were used: 5'-GTATGGCAGCAACGTCACGA-3' and 5'-GCTTGCGTTAGTGGTGTACT-3', synthesized by Microsynth (Balgach, Switzerland). The sgRNA sequences were cloned into vectors.²⁴ The pSpCas9 (BB)-2A-GFP (PX458) plasmid, containing Cas9 endonuclease and green fluorescent protein (GFP), was a gift from Dr. F. Zhang (Addgene plasmid # 48138, Teddington, UK). The final constructs were transfected into CT-2A, SMA-560, and GL-261 cells with TransIT-X2 (Mirus Bio, Madison, WI). At 24 h after transfection, single GFP-positive cells were sorted into 96-well plates by the use of BD FACSAria III cell sorter (BD Biosciences, Allschwil, Switzerland). Clones were screened for the absence of protein by flow cytometry and at genomic level by lack of amplification of mRNA of the predicted knockout site by reverse transcriptase quantitative polymerase chain reaction (RT-qPCR) with primers aligning to predicted sgRNA break sites.

Material and Methods

Cell Lines

SMA-497, SMA-540, and SMA-560 cells were obtained from Dr. D. Bigner (Duke, NC). GL-261 cells were obtained from the National Cancer Institute (Frederick, MD). The CT-2A cell line was purchased from Merck/Sigma-Aldrich (SCC194, Darmstadt, Germany). All cells were maintained in Dulbecco's modified Eagle medium (DMEM)

Cell Growth and Clonogenicity

Clonogenic survival was measured by limiting dilution assays. For each cell line, sextuplicates were prepared in serial dilutions ranging from 500 cells/well to 1 cell/well. At day 10 or later depending on the cell line, the wells were stained for 10 min with crystal violet (C2886, Sigma), and absorbance was measured and quantified by Infinite M200 Pro plate-reader (Tecan Life Sciences, Männedorf, Switzerland).

Reverse Transcription qPCR

Total RNA was isolated with the NucleoSpin column system (Macherey-Nagel AG, Oensingen, Switzerland) and transcribed into cDNA by using a High-Capacity cDNA Reverse Transcription Kit (Applied Biosystems by Thermo Fisher Scientific, Waltham, MA). Gene expression was quantified by PowerUp SYBR Green master mix (Applied Biosystems by Thermo Fisher Scientific) in a QuantStudio 6 Flex Real-Time PCR system (Applied Biosystems). The following primers (Microsynt AG) were used: mouse *Hprt1*: forward 5'-TTGCTGACCTGCTGGATTAC-3', reverse 5'-TTTATGTCCCCGTTGACTG-3', mouse *Pd-11*: forward 5'-TGCGGACTACAAGCGAATCA-3', reverse 5'-GATCCACGGAAATTCTCTGGTT-3', *Pd-12*: forward 5'-GTGCTGGGTGCTGATATTGAC-3', reverse 5'-AAAATCGCACTCCAGGCTCA-3', mouse *Pd-11* for CRISPR validation: forward 5'-AGCAACGTCACGATGGAGTG-3', reverse 5'-TCCCAGTACACCACTAACGC-3'. The PCR conditions were as follows: 40 cycles, 95°C 15 s, 60°C 1 min. Relative gene expression was calculated using the $2^{(-\Delta\Delta CT)}$ method using *Hprt1* expression for normalization.²⁵

Flow Cytometry

Cells were detached and dissociated with accutase (Thermo Fisher Scientific) and subsequently incubated with fluorescently labeled primary antibodies and viability dye for 30 min at 4°C. Fluorescence was detected with a BD FACSVerser flow cytometer (BD Biosciences). Data analysis was made with FlowJo (TreeStar, Ashland, OR). Dead cells were gated out by positivity for staining with Zombie viability dye (Aqua, Violet or NIR depending on the fluorochrome combination, 1:1000 BioLegend, San Diego, CA). Specific fluorescence indices (SFI) were calculated as the ratio between median fluorescence of specific and isotype antibodies. Conjugated antibodies were used as follows: BV421 rat anti-mouse PD-L1 (clone MIH5, 1:50, BD Biosciences) and APC rat anti-mouse PD-L2 (clone TY25, 1:50, BD Biosciences). Isotype controls were used at the same concentrations as the corresponding specific antibodies: BV421 rat IgG2a, λ isotype control (clone B39-4, BD Biosciences), APC rat IgG2a κ isotype control (clone R35-95m, BD Biosciences).

Co-culture Experiments

A detailed description of co-culture methodology and conditions can be found in [Supplementary Note 1](#).

Animal Experiments

Wild-type C57BL/6 mice were purchased from Janvier Labs (Le Genest-Saint-Isle, France). RAG^{-/-} mice were bred at the University of Zurich in pathogen-free facilities. The mice underwent surgery at age 6-12 weeks. Stereotactic intracranial tumor cell implantation was made into the right striatum; 80,000 cells were implanted for CT-2A, 100,000 cells were implanted for GL-261, and 20,000 cells were implanted for SMA-560. Mice were regularly monitored and

ethanized as indicated or when developing neurological symptoms grade 2; weight loss above 15% compared with weight at day of tumor cell implantation, moderate signs of pain, slight paralysis of left leg or no/decreased activity. Where indicated, mice received anti-PD-L1 (Genentech Clone 6E11) twice weekly, 5 mg/kg intra-peritoneally. Treatments were started 5 days after tumor cell implantation. Anti-PD-L1 treatment was given for 3 consecutive weeks. All animal study procedures were approved by Swiss Cantonal Veterinary office under animal licenses ZH098/2018 and ZH109/2020.

Histology

Immunohistochemistry was performed as previously described.²⁶ Primary antibodies used for stainings were as follows: anti-PD-1 (135203, clone 29F1A12, 1:200, BioLegend), anti-PD-L1 (153602, clone MIH6, 1:200, BioLegend), anti-Ki67 (DRM004, 1:100, Origene, Rockville, MD), anti-CD3 (555273, clone 17A2, 1:100, BD Pharmingen), anti-CD11b (550282, 1:500, BD Pharmingen), and anti-CD45 (103102, clone 30-F11, 1:500, BioLegend). DAB staining intensity quantification was made with ImageJ.²⁷

Statistical Analysis

Data are represented as mean and standard deviation (SD). Graphs show representative experiments. GraphPad Prism 8 (GraphPad Software, San Diego, CA) was used for statistical analysis. To test for differences between 2 groups, unpaired *t*-test assuming equal SD was used. For experiments with more than 2 groups and paired samples, 1- or 2-way ANOVA was used with Tukey's post hoc test to adjust for multiple testing. Survival data were analyzed by Kaplan-Meier survival curves, significance was tested using the log-rank test. Significance is denoted as **p* < .05; ***p* < .01; ****p* < .001.

Results

PD Ligand Expression in Murine Glioma Cells In Vitro and In Vivo

Relative to splenocytes, constitutive levels of *Pd11* mRNA were low in the mouse glioma cell lines, with highest expression in CT-2A and GL-261 cells, which also showed PD-L1 protein at the cell surface by flow cytometry ([Figure 1A](#) and [B](#)). *Pd12* mRNA was detected only in SMA-497 cells, albeit at expression values close to the reliability threshold defined by a CT value above 32. Cell surface protein levels of PD-L2 were below detection limit by flow cytometry ([Figure 1C](#) and [D](#)). None of the 5 cell lines expressed mRNA for the receptor *Pdcd1*, using splenocytes as a positive control (data not shown). PD-L1 protein was detected by immunohistochemistry in the tumors of 4 of the 5 syngeneic mouse glioma models examined, namely CT-2A, SMA-497, SMA-540, and GL-261. Despite low-level protein detected in vitro, SMA-560 tumor cells showed no staining for PD-L1 protein in vivo ([Figure 1E](#)). The frequency of

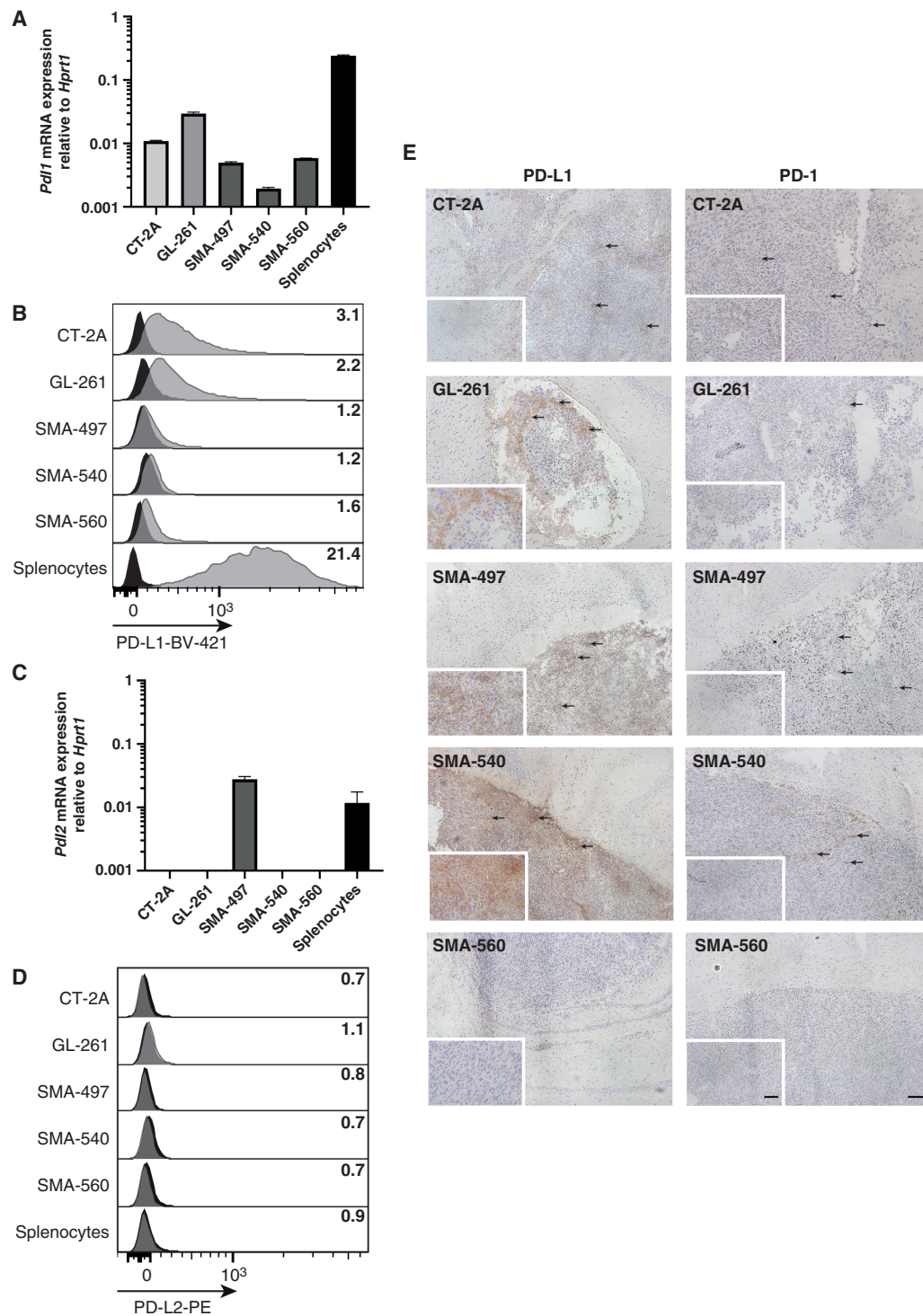


Figure 1. PD-L1 and PD-L2 expression in murine glioma models in vitro and in vivo. (A–D) Relative *Pdl1* and *Pdl2* mRNA expression were determined by RT-qPCR using *Hprt1* as a reference gene (A, C). PD-L1 and PD-L2 surface protein levels were determined by flow cytometry. Black histograms represent isotype control antibody staining whereas gray represents experimental antibody staining. (B, D). E, F. PD-L1 (E) and PD-1 (F) protein was assessed by immunohistochemistry in brains of tumor-bearing mice. 10 \times magnification was used for an overview, stained cells are exemplified by arrows and a scale bar of 100 μ m is included in the bottom right corner of the figure panel. 40 \times magnification was used for the inserts with a scale bar of 50 μ m in the bottom right corner of the figure panel.

PD-1-positive host cells followed a similar pattern as for the PD-L1 staining, with SMA-497, SMA-540, and CT-2A having more stained cells, whereas GL-261 had only few stained cells and no stained cells were detected in SMA-560 (Figure 1F).

PD Ligand Induction by IFN and Co-culture With Splenocytes

PD-L1 expression was highly inducible by IFN- γ and to a lesser extent by IFN- β in all glioma cell lines except CT-2A, which was relatively more responsive to IFN- β (Figure 2A and C). *Pdl2* mRNA was not increased or induced upon IFN stimulation (Figure 2B, and PD-L2 protein was still not detected in any cell line even after IFN stimulation (data not shown). Since the protein levels of PD-L1 in glioma cells in vivo did not correspond well with the RT-qPCR and flow cytometry data in vitro, we reasoned that the upregulation of PD-L1 in vivo could be induced by factors or cells present in the tumor microenvironment. To first test this notion in vitro, co-culture experiments were performed. Glioma cells were stained with a membrane dye to be able to specifically monitor their PD-L1 protein levels. Labeled glioma cells were incubated together with splenocytes for 24 h. Thereafter, PD-L1 protein levels were determined after first gating on single live glioma cells (Figure 3A). Indeed, a strong upregulation of PD-L1 surface protein was detected on 2 of 3 glioma cell lines upon co-culture with splenocytes (Figure 3B). Because of the strong induction of PD-L1 protein in GL-261 and SMA-560 cells, we hypothesized that the induction was due to release of IFN- γ by activated splenocytes in the co-culture. This phenomenon could also be occurring in the microenvironment of the mice and explain immune cell mediated increase of PD-L1 in vivo. Indeed, exposure to a neutralizing IFN- γ -R1 antibody abrogated the effector:target ratio-dependent induction of PD-L1 on the glioma cells (Figure 3C).

Generation and Characterization of PD-L1-Deficient Glioma Cell Lines

To study the role of PD-L1 expression by mouse glioma cells further, PD-L1-deficient cell lines were generated using CRISPR/Cas9 technology (Supplementary Figure S1A). Primers that align to the predicted cut sites were used to assess *Pdl1* gene disruption and absence of surface protein levels was confirmed by flow cytometry (Supplementary Figure S1B and C). Furthermore, only CRISPR control cells upregulated PD-L1 protein in response to IFN- γ , whereas the knockout sublines remained negative for PD-L1 protein (Figure 4A). This finding was confirmed by immunocytochemistry using an antibody recognizing another epitope of PD-L1. PD-L1 induction upon IFN- γ stimulation was again only seen in CRISPR control cells (Figure 4B). No change of growth under standard culture conditions assessed by doubling times (data not shown) or in serial dilution assays (Figure 4C) was observed upon PD-L1 gene disruption in either of the cell lines. Co-culture assays of CRISPR control or PD-L1 knockout cells with syngeneic splenocytes revealed overall minor changes with clonal variation, but no

clear-cut increase in sensitivity to lysis mediated by PD-L1 loss (Supplementary Figure S1D).

Characterization of PD-L1 Knockout Glioma Cell Models In Vivo

To further elucidate the role of PD-L1 expression in murine glioma models, CRISPR control or PD-L1 knockout glioma cells were implanted into the brains of syngeneic recipient mice. PD-L1-deficient GL-261 and SMA-560 cells showed no difference in survival compared with wild-type or control cells (Supplementary Figure S2). In contrast, mice inoculated with CT-2A cells deficient for PD-L1 experienced a survival benefit compared with controls (Figure 5A). Histological studies at early tumor stages showed no significant differences in tumor size (Figure 5B) and no difference in Ki67 labeling (Figure 5C). PD-L1 was detected at similar levels in all tumors, however, PD-L1-positive staining in PD-L1 knockout tumors co-localized with CD45 staining, suggesting a PD-L1-positive immune cell presence. Conversely, in control tumors, PD-L1 staining was also seen in areas lacking CD45 expression. There was a trend for higher frequency of CD45-positive cells in PD-L1 knockout tumors; however, the number of CD3-positive cells remained low. CD11b staining largely coincided with CD45 staining, indicating a substantial innate immune presence (Figure 5C).

To confirm the importance of glioma-expressed PD-L1 protein in vivo, an anti-PD-L1 antibody was used to treat mice bearing either CRISPR control or PD-L1 knockout CT-2A tumors. Anti-PD-L1 treatment conferred a survival benefit only in mice bearing PD-L1-proficient tumors, in contrast, mice bearing PD-L1 knockout tumors did not benefit from this treatment (Figure 6A). Next, the role of B and T cells in glioma growth were assessed using RAG^{-/-} mice which lack these 2 cell types. CRISPR control or PD-L1 knockout cells were implanted in RAG^{-/-} mice. The PD-L1 knockout in the CT-2A model conferred a significant survival benefit also in the immunodeficient mice (Figure 6B). To evaluate whether the conferred survival benefit seen with anti-PD-L1 treatment was T cell dependent, wild-type CT-2A cells were implanted in RAG^{-/-} mice and subsequently treated with anti-PD-L1 antibody. No survival benefit was observed upon administration of anti-PD-L1 treatment (Figure 6C).

Discussion

Since the introduction of temozolomide to the standard of care in 2005,²⁸ no major advancements in the systemic treatment of glioblastoma have been made.¹ The disease remains uniformly lethal despite substantial research efforts and numerous completed clinical trials from various areas, notably angiogenesis inhibition and immunotherapy. The immune cell compartment of glioblastoma constitutes a major part of the tumor microenvironment, albeit mostly of myeloid lineage.²⁹⁻³¹ Thus, although numerous immune cells are present, glioma cells have found a way to escape immune surveillance.³² Because of its

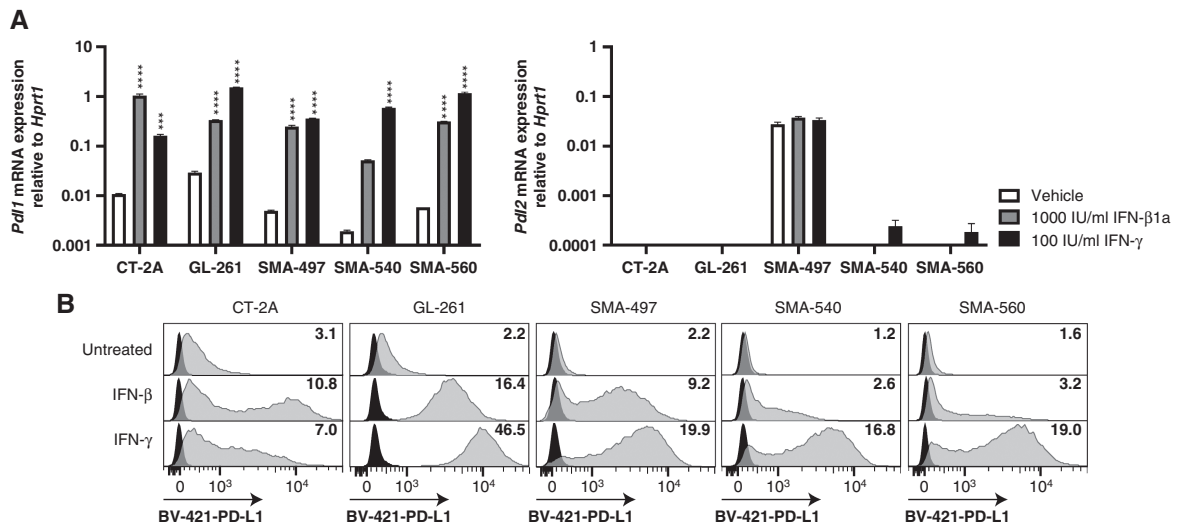


Figure 2. PD-L1 is inducible by IFN- β and IFN- γ . *Pd1* and *Pd2* mRNA expression (A, B) and PD-L1 protein (C) were assessed by RT-qPCR or flow cytometry after exposure to IFN- β 1a (1000 U/ml, 24 h) or to IFN- γ (100 U/ml, 24 h), untreated being the same measurement as in Figure 1. *Hprt1* was used as a reference gene for RT-qPCR, and an isotype control antibody was used as a reference for flow cytometry (black histograms). mRNA data are represented as mean and SD (2-way ANOVA with Tukey's post hoc test for multiple comparison, *** $p < .001$, **** $p < .0001$). Protein levels are expressed as SFI values relative to an isotype control antibody (black histograms).

success in other malignancies with poor prognosis, immunotherapy has also been extensively investigated in glioblastoma, including vaccines,³³ antibody drug conjugates,³⁴ and immune checkpoint inhibition.^{35–37} So far, the efficacy of immunotherapy remains poor in glioblastoma.

Here we explored the consequences of *Pd1* gene disruption in commonly used murine glioma models. We found that all mouse glioma cell lines expressed PD-L1, but not PD-L2. The current study suggests that, in the CT-2A model, elimination of PD-L1 on the tumor cells conferred a survival benefit that was comparable to the survival benefit seen by pharmacological intervention. Since the survival gain afforded by PD-L1 loss persisted when tumor cells were implanted into immune deficient RAG^{-/-} mice, we concluded that infiltrating B and T cells cannot be the effector cells mediating the survival benefit seen in WT mice inoculated with PD-L1 knockout tumor cells. One another possible explanation for this is the notion that ablating PD-L1 has an intrinsic effect on glioma cells that does not become apparent in vitro. Limited data have been published since the initial finding that PD-L1 could have intrinsic backward signaling effects on cancer cells in 2016.²² However, this would explain why no further effect was seen when anti-PD-L1 treatment was given to mice bearing PD-L1 knockout tumors. Although little is known about intrinsic cancer cell signaling upon binding an anti-PD-L1 antibody, one study has demonstrated sensitization to interferon beta in 4 different cancer cell lines when co-treated with anti-PD-L1 antibody.³⁸ Although we did not observe IFN sensitization in our system upon *Pd1* knockout in vitro (data not shown), this does not rule out modulation of other intrinsic pathways upon PD-L1 antibody binding.

Systemic anti-PD-L1 monotherapy has been tested in various preclinical glioma models previously. It significantly

prolonged survival in GL-261,^{39–41} a stem cell-derived glioma model (005 GSC)⁴² and in CT-2A.⁴¹ The CT-2A model was, in accordance to the previous literature, also responsive to the specific anti-PD-L1 clone used in our experiments. We confirmed that PD-L1 knockout tumors still harbor PD-L1-positive immune cells; however, when these cells are pharmacologically blocked by anti-PD-L1 treatment, there appears to be no additional survival benefit.

This contrasts with other tumor models, for example, ovarian cancer, melanoma, and colon cancer, where mice still benefited from anti-PD-L1 treatment in the absence of PD-L1 expression in the tumor.^{43,44} Interestingly, however, the effect of anti-PD-L1 treatment was abolished when the host was PD-L1 deficient,⁴⁴ reinvigorating the potential immune sanctuary of the brain as a cause of these contrasting observations.

We confirmed that the anti-PD-L1 treatment effect is indeed T or B cell dependent since it was abrogated in RAG^{-/-} mice; however, CT-2A PD-L1 KO cells still demonstrated significant survival benefit in RAG^{-/-} mice. We therefore conclude that PD-L1 knockout in CT-2A confers a decrease in tumor growth, which is T and B cell independent, and cannot be augmented with anti-PD-L1 treatment. Further studies including ex vivo omics approaches, not only limited to one time point, will be required to understand the intrinsic or microenvironment dependent factors that cause this immune independent change in tumor growth. For example, IL-6 is a known inducer of PD-L1 on myeloid cells in preclinical glioma models and its expression could potentially be altered in the PD-L1 deficient tumors.⁴⁵

Although multiple preclinical models have demonstrated significant survival benefit of anti-PD-L1 treatment,^{39,40,42} this has not been substantiated in clinical trials. Two phase II anti-PD-L1 clinical trials have been performed

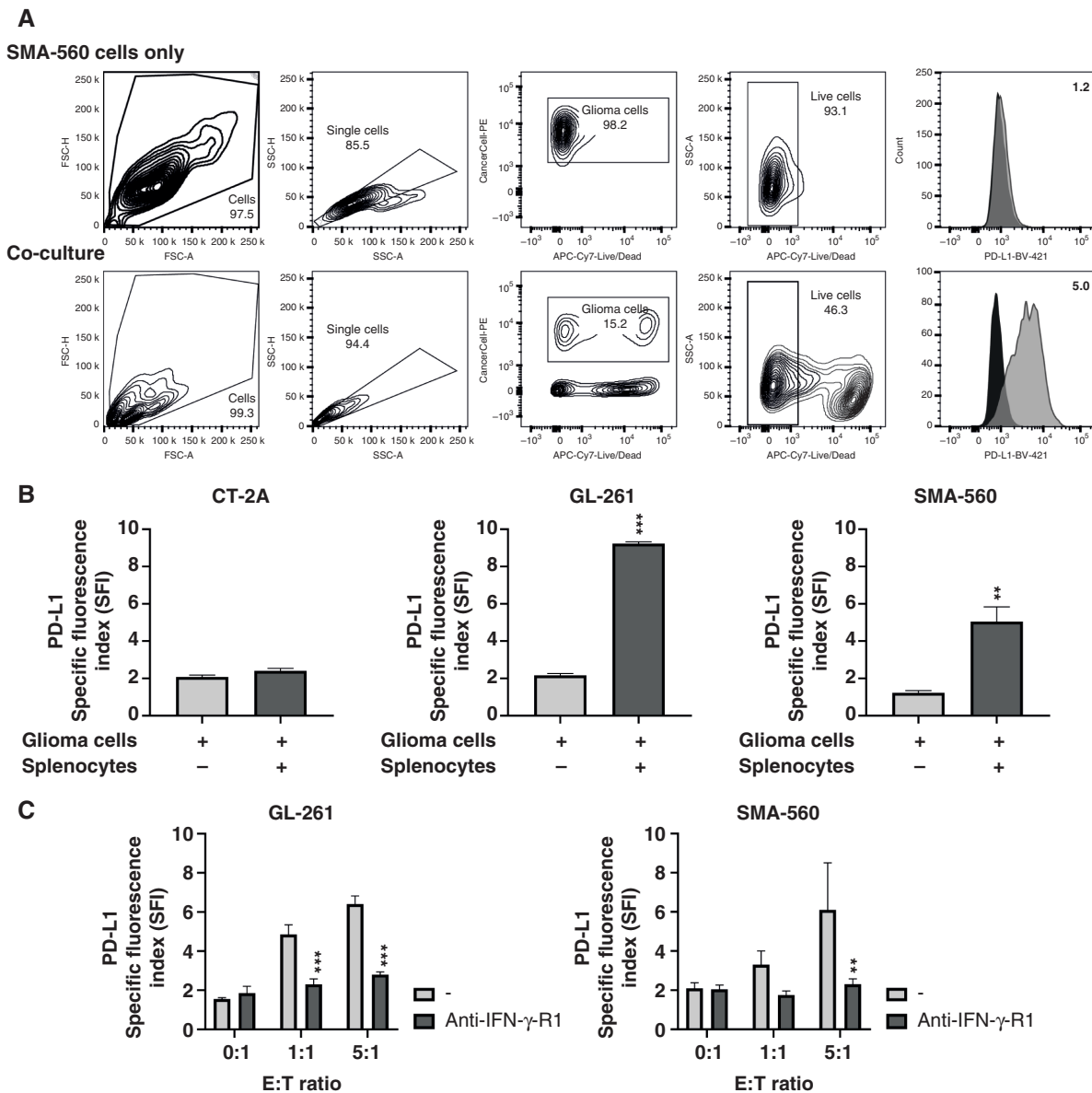


Figure 3. PD-L1 is upregulated when co-cultured with splenocytes in a IFN- γ -dependent manner. (A) Gating strategy used to ensure glioma cell-specific PD-L1 protein assessment. Glioma cells were stained with a membrane dye and then either cultured alone or together with splenocytes in a 10:1 effector:target ratio for 24 h. Thereafter, the cells were stained with isotype control antibody (black) or PD-L1 antibody (gray). (B) Quantification of PD-L1 protein levels normalized to isotype control staining on glioma cells cultured alone or together with splenocytes (E:T 5:1, 24 h). (C) Similar studies as in (B), but IFN- γ -R1 antibody (10 ng/ml) was added to the co-culture of 24 h where indicated. PD-L1 protein levels were quantified by flow cytometry, normalized to an isotype control, and quantified by SFI values. Data are represented as mean and SD (unpaired *t*-test assuming equal SD, ***p* < .01, ****p* < .001).

in glioblastoma. No clinical efficacy, in either primary or recurrent glioblastoma patients cohorts, was observed; however, PD-L1 levels were not investigated in these patients and its relevance for clinical outcome could therefore not be determined.^{46,47}

Trials in other cancer entities have investigated PD-L1 on tumor and immune cells separately to understand their contribution to the response to anti-PD-L1 treatment. In a meta-analysis of multiple clinical trials in patients with

non-small cell lung cancer, there were tumors with PD-L1 expressed on tumor cells or immune cells only, but PD-L1 protein expressed in either compartment was associated with response to anti-PD-L1 treatment. However, response to anti-PD-L1 treatment was higher with PD-L1 expressed on tumor cells than on immune cells.⁴⁸

The main general limitation of our study include the incomplete reproduction of human glioblastoma by our standard murine glioma models. Furthermore, clonal

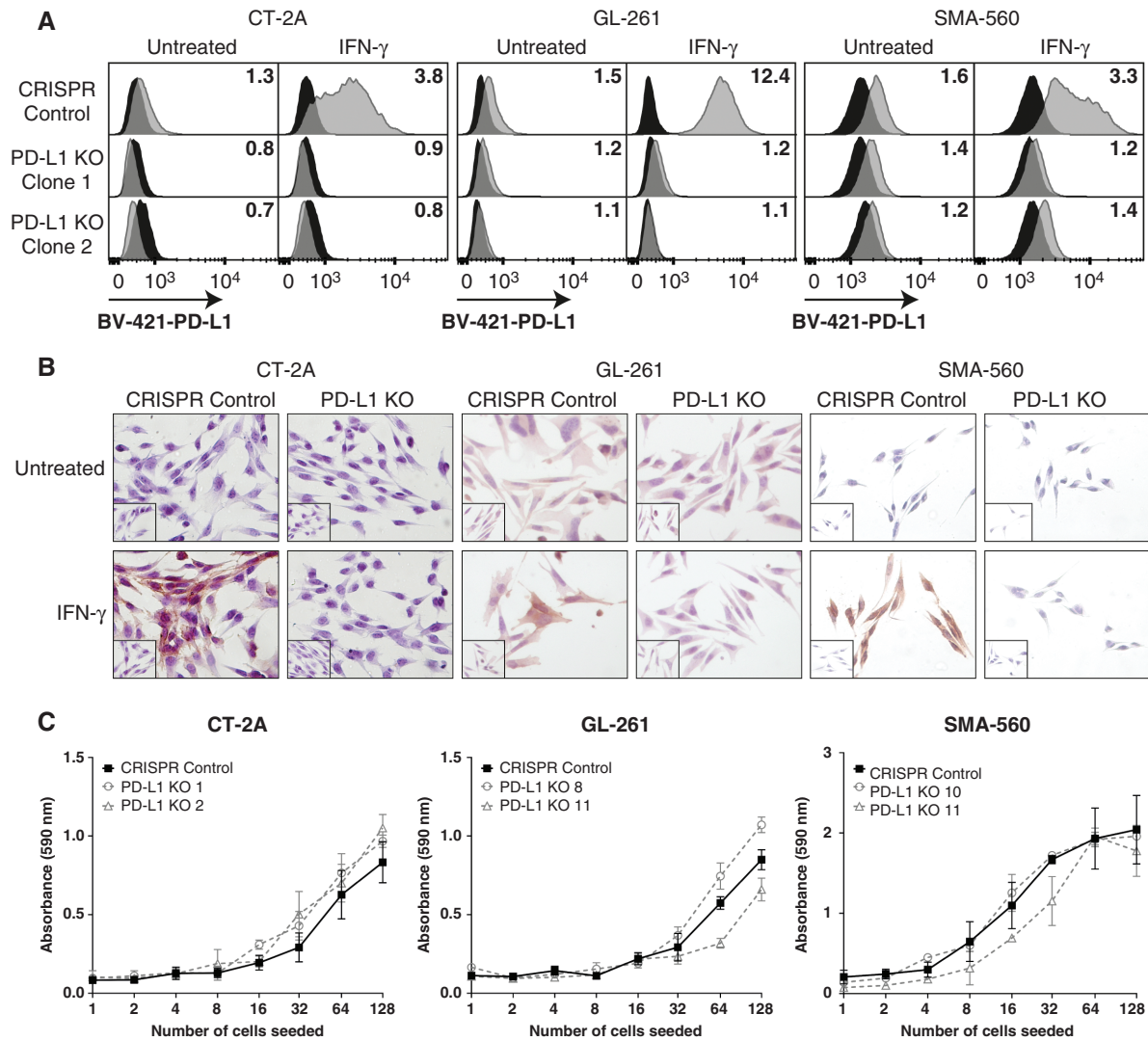


Figure 4. PD-L1 knockout does not generate a phenotype in vitro. (A) PD-L1 protein levels were assessed by flow cytometry after exposure to IFN- γ (150 U/ml, 24 h). Protein levels are expressed as SFI values relative to an isotype control antibody (black histograms). (B) PD-L1 protein induction was assessed by immunohistochemistry after exposure to IFN- γ (150 U/ml, 24 h). Photographs were taken with 40 \times magnification. Inserts depict parallel samples stained with isotype control antibody. Scale bar represents 100 μ m. (C) CRISPR control or PD-L1 KO cells were seeded in serial dilutions. The cells were incubated for 7–10 days to determine cell growth. At the end point, the wells were stained with crystal violet and absorbance was measured at 590 nm.

artifacts are an inherent risk using CRISPR Cas9 technology, but these were minimized by generating several subclones for each model. The divergent observations in various models are not a limitation, but merely illustrate that the relevance of PD-L1 for tumor immunobiology is model-specific. Finally, it remains unclear whether the protumorigenic role of PD-L1 in the CT-2A model depends on interactions of PD-L1 with non-lymphocyte PD-1 expressing target cells or on backward signaling (Figure 6).

Our findings may be considered compatible with the failure of 3 phase III clinical trials testing the efficacy of anti-PD-1 treatment in recurrent (CheckMate 143)³⁵ and newly diagnosed (CheckMate 498),³⁷ (CheckMate 548)³⁶ glioblastoma as well as 2 phase II trials testing the

efficacy of anti-PD-L1 treatment in newly diagnosed glioblastoma.^{46,47} Further studies may need to explore combinatorial approaches of immunotherapy,⁴⁹ potentially exploiting the “priming” for surgery advocated by the “neoadjuvant” presurgical approach,⁵⁰ and novel strategies to allow peripheral PD-L1 blockade to be translated into improved immune responsiveness in the brain tumor microenvironment.

Supplementary Material

Supplementary material is available at *Neuro-Oncology Advances* online.

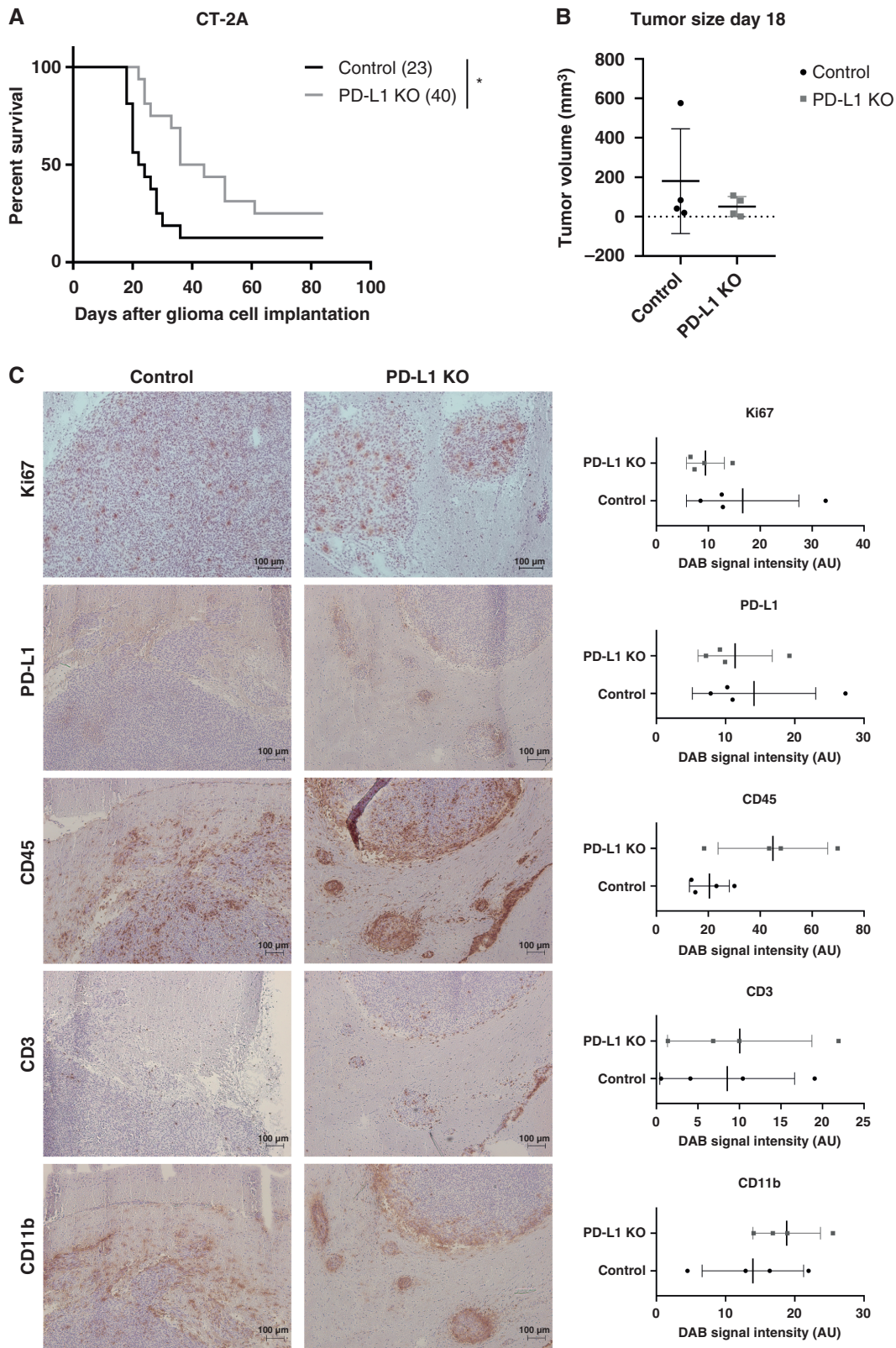


Figure 5. PD-L1 knockout confers a survival benefit in the CT-2A model. (A) CT-2A control (WT and CRISPR control grouped together) or PD-L1 KO (PD-L1 KO clone 1 or 2 grouped together) were orthotopically implanted in C57BL/6 mice (for each combined group $n = 14$). Survival data are presented as Kaplan–Meier plots (log-rank test, $*p < .05$). Median survival (days) is indicated within brackets in legend. (B) Tumor volumes were calculated on the basis of H&E sections of the whole tumor ($n = 4$). (C) Immunohistochemical staining of CT-2A control or PD-L1 KO tumors. Scale bar represents 100 μm . Quantification of DAB signal intensity was performed and represented in graphs to the right ($n = 4$).

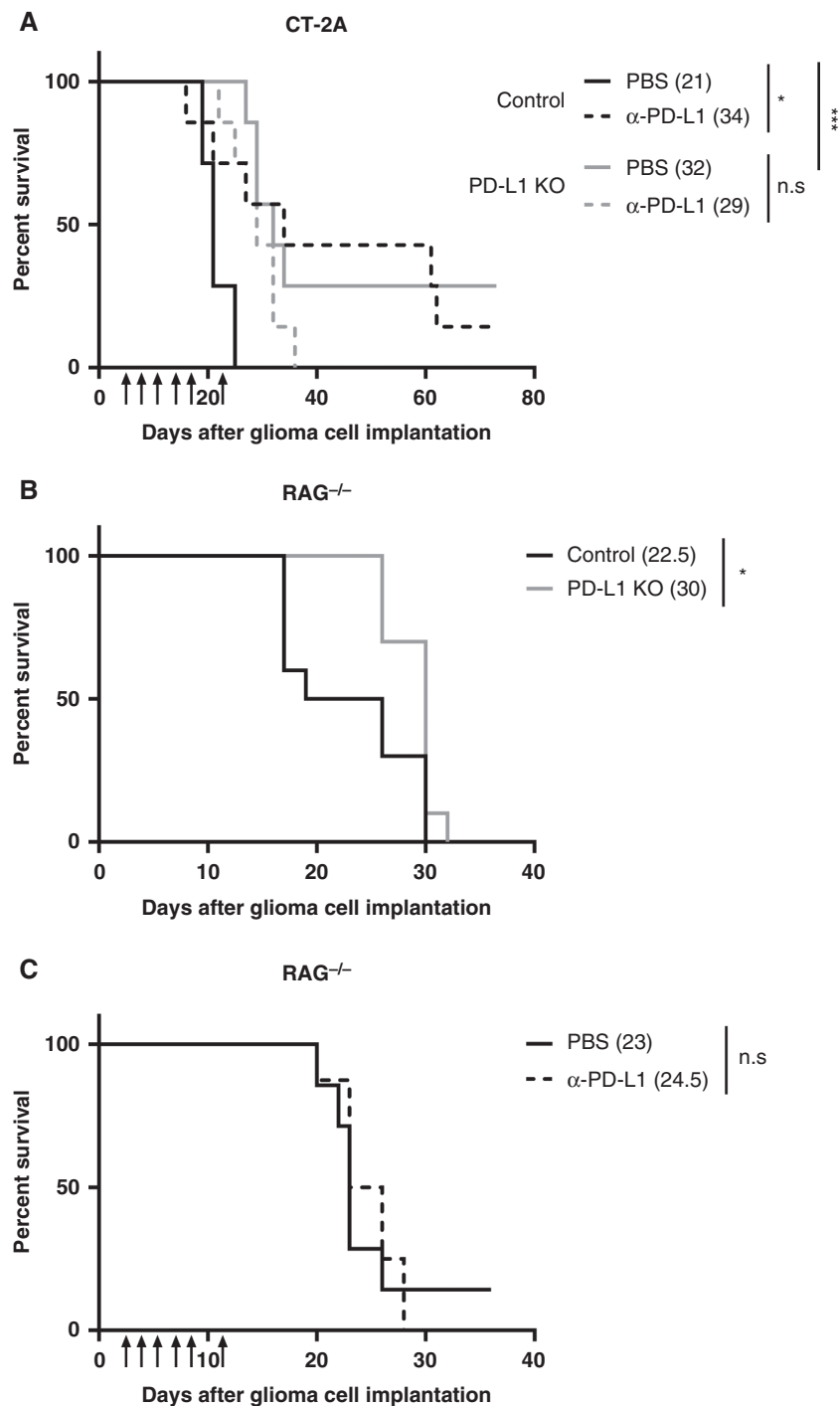


Figure 6. PD-L1 tumor knockout abrogates response to anti-PD-L1 treatment, but the effect is T cell mediated. (A) CT-2A control or PD-L1 KO cells were orthotopically implanted in C57BL/6 mice (for each group $n = 7$). Tumor-bearing mice were treated 6 times with PBS or an anti-PD-L1 antibody (5 mg/kg, i.p., twice weekly, starting at day 5). (B) CT-2A WT, CRISPR control (grouped as control), PD-L1 KO clone 1 or 2 (grouped as PD-L1 KO) were orthotopically implanted in RAG^{-/-} C57BL/6 mice (for each group $n = 7$). (C) CT-2A WT cells were implanted were orthotopically implanted in RAG^{-/-} C57BL/6 mice (for each group $n = 7$). Tumor-bearing mice were treated 6 times with PBS or an anti-PD-L1 antibody (5 mg/kg, i.p., twice weekly, starting at day 5). Survival data are presented as Kaplan–Meier plots (log-rank test, * $p < .05$, *** $p < .001$). Median survival (days) is indicated within brackets in legend.

Keywords

glioblastoma | immune checkpoint inhibition | immunosuppression | immunotherapy | PD-L1

Funding

Swiss National Science Foundation (310030_185155/1) to M.W., the Detas Foundation, and the Clinical Research Priority Program (CRPP) of the University of Zurich for the CRPP ImmunoCure.

Acknowledgments

The authors thank Julia Friesen, Sujani Neranjan, and Anna Hübner for excellent technical assistance.

Conflict of interest statement. E.B. reports no conflicts of interest. M.S. reports no conflicts of interest. P.R. has received honoraria for lectures or advisory board participation from Bristol-Myers Squibb, Boehringer Ingelheim, Debiopharm, Merck Sharp and Dohme, Novocure, QED, and Roche and research support from Merck Sharp and Dohme and Novocure. M.W. has received research grants from Apogenix, Merck, Sharp & Dohme, Merck (EMD), Philogen and Quercis, and honoraria for lectures or advisory board participation or consulting from Adastra, Bayer, Bristol Meyer Squibb, Medac, Merck, Sharp & Dohme, Merck (EMD), Nerviano Medical Sciences, Novartis, Orbus, Philogen, and γ-Mabs.

Authorship statement

Experimental design and implementation (E.B., M.S., and M.W.), analysis, interpretation of the data and reviewing the manuscript (E.B., M.S., P.R., and M.W.), and writing of the original manuscript draft (E.B., M.W.).

References

- Weller M, van den Bent M, Preusser M, et al. EANO guidelines on the diagnosis and treatment of diffuse gliomas of adulthood. *Nat Rev Clin Oncol*. 2021;18(3):170–186.
- Ostrom QT, Cioffi G, Waite K, Kruchko C, Barnholtz-Sloan JS. CBTRUS statistical report: primary brain and other central nervous system tumors diagnosed in the United States in 2014–2018. *Neuro-oncology*. 2021;23(12 Suppl 2):iii1–iii105.
- Gramatzki D, Dehler S, Rushing EJ, et al. Glioblastoma in the Canton of Zurich, Switzerland revisited: 2005 to 2009. *Cancer*. 2016;122(14):2206–2215.
- Lim M, Xia Y, Bettgowda C, Weller M. Current state of immunotherapy for glioblastoma. *Nat Rev Clin Oncol*. 2018;15(7):422–442.
- Keir ME, Butte MJ, Freeman GJ, Sharpe AH. PD-1 and its ligands in tolerance and immunity. *Annu Rev Immunol*. 2008;26:677–704.
- Waldman AD, Fritz JM, Lenardo MJ. A guide to cancer immunotherapy: from T cell basic science to clinical practice. *Nat Rev Immunol*. 2020;20(11):651–668.
- Pardoll DM. The blockade of immune checkpoints in cancer immunotherapy. *Nat Rev Cancer*. 2012;12(4):252–264.
- Blank C, Gajewski TF, Mackensen A. Interaction of PD-L1 on tumor cells with PD-1 on tumor-specific T cells as a mechanism of immune evasion: implications for tumor immunotherapy. *Cancer Immunol Immunother*. 2005;54(4):307–314.
- Hodi FS, O'Day SJ, McDermott DF, et al. Improved survival with ipilimumab in patients with metastatic melanoma. *N Engl J Med*. 2010;363(8):711–723.
- Le DT, Durham JN, Smith KN, et al. Mismatch repair deficiency predicts response of solid tumors to PD-1 blockade. *Science (New York, N.Y.)*. 2017;357(6349):409–413.
- Yarchoan M, Hopkins A, Jaffee EM. Tumor mutational burden and response rate to PD-1 inhibition. *N Engl J Med*. 2017;377(25):2500–2501.
- Antonios JP, Soto H, Everson RG, et al. Immunosuppressive tumor-infiltrating myeloid cells mediate adaptive immune resistance via a PD-1/PD-L1 mechanism in glioblastoma. *Neuro-Oncology*. 2017;19(6):796–807.
- Wilmotte R, Burkhardt K, Kindler V, et al. B7-homolog 1 expression by human glioma: a new mechanism of immune evasion. *Neuroreport*. 2005;16(10):1081–1085.
- Chen RQ, Liu F, Qiu XY, Chen XQ. The prognostic and therapeutic value of PD-L1 in glioma. *Front Pharmacol*. 2019;9:1503–1503.
- Wang Z, Zhang C, Liu X, et al. Molecular and clinical characterization of PD-L1 expression at transcriptional level via 976 samples of brain glioma. *Oncotarget*. 2016;5(11):e1196310.
- Nduom EK, Wei J, Yaghi NK, et al. PD-L1 expression and prognostic impact in glioblastoma. *Neuro-Oncology*. 2016;18(2):195–205.
- Lee KS, Lee K, Yun S, et al. Prognostic relevance of programmed cell death ligand 1 expression in glioblastoma. *J Neurooncol*. 2018;136(3):453–461.
- Pratt D, Dominah G, Lobel G, et al. Programmed death ligand 1 is a negative prognostic marker in recurrent isocitrate dehydrogenase-wildtype glioblastoma. *Neurosurgery*. 2019;85(2):280–289.
- Berghoff AS, Kiesel B, Widhalm G, et al. Programmed death ligand 1 expression and tumor-infiltrating lymphocytes in glioblastoma. *Neuro-Oncology*. 2015;17(8):1064–1075.
- Zeng J, Zhang XK, Chen HD, et al. Expression of programmed cell death-ligand 1 and its correlation with clinical outcomes in gliomas. *Oncotarget*. 2016;7(8):8944–8955.
- Miyazaki T, Ishikawa E, Matsuda M, et al. Assessment of PD-1 positive cells on initial and secondary resected tumor specimens of newly diagnosed glioblastoma and its implications on patient outcome. *J Neurooncol*. 2017;133(2):277–285.
- Clark CA, Gupta HB, Sareddy G, et al. Tumor-intrinsic PD-L1 signals regulate cell growth, pathogenesis, and autophagy in ovarian cancer and melanoma. *Cancer Res*. 2016;76(23):6964–6974.
- Chen L, Xiong Y, Li J, et al. PD-L1 expression promotes epithelial to mesenchymal transition in human esophageal cancer. *Cell Physiol Biochem*. 2017;42(6):2267–2280.
- Ran FA, Hsu PD, Wright J, et al. Genome engineering using the CRISPR-Cas9 system. *Nat Protoc*. 2013;8(11):2281–2308.
- Livak KJ, Schmittgen TD. Analysis of relative gene expression data using real-time quantitative PCR and the 2⁻(Delta Delta C(T)) method. *Methods*. 2001;25(4):402–408.

26. Papachristodoulou A, Silginer M, Weller M, et al. Therapeutic targeting of TGF β ligands in glioblastoma using novel antisense oligonucleotides reduces the growth of experimental gliomas. *Clin Cancer Res*. 2019;25(23):7189–7201.
27. Crowe AR, Yue W. Semi-quantitative determination of protein expression using immunohistochemistry staining and analysis: an integrated protocol. *Bio Protoc*. 2019;9(24):e3465.
28. Stupp R, Mason WP, van den Bent MJ, et al. Radiotherapy plus concomitant and adjuvant temozolomide for glioblastoma. *N Engl J Med*. 2005;352(10):987–996.
29. Hambardzumyan D, Gutmann DH, Kettenmann H. The role of microglia and macrophages in glioma maintenance and progression. *Nat Neurosci*. 2016;19(1):20–27.
30. Friebel E, Kapolou K, Unger S, et al. Single-cell mapping of human brain cancer reveals tumor-specific instruction of tissue-invading leukocytes. *Cell*. 2020;181(7):1626–1642.e20.
31. Klemm F, Maas RR, Bowman RL, et al. Interrogation of the microenvironmental landscape in brain tumors reveals disease-specific alterations of immune cells. *Cell*. 2020;181(7):1643–1660.e17.
32. Mangani D, Weller M, Roth P. The network of immunosuppressive pathways in glioblastoma. *Biochem Pharmacol*. 2017;130:1–9.
33. Weller M, Butowski N, Tran DD, et al. Rindopepimut with temozolomide for patients with newly diagnosed, EGFRvIII-expressing glioblastoma (ACT IV): a randomised, double-blind, international phase 3 trial. *Lancet Oncol*. 2017;18(10):1373–1385.
34. Van Den Bent M, Eoli M, Sepulveda JM, et al. INTELLANCE 2/ EORTC 1410 randomized phase II study of Depatux-M alone and with temozolomide vs temozolomide or lomustine in recurrent EGFR amplified glioblastoma. *Neuro-Oncology*. 2020;22(5):684–693.
35. Reardon DA, Brandes AA, Omuro A, et al. Effect of Nivolumab vs Bevacizumab in patients with recurrent glioblastoma: the checkmate 143 phase 3 randomized clinical trial. *JAMA Oncol*. 2020;6(7):1003–1010.
36. Lim M, Weller M, Idbaih A, et al. Phase 3 trial of chemoradiotherapy with temozolomide plus nivolumab or placebo for newly diagnosed glioblastoma with methylated MGMT promoter. *Neuro-Oncology*. 2022:noac116.
37. Omuro A, Brandes AA, Carpentier AF, et al. Radiotherapy combined with nivolumab or temozolomide for newly diagnosed glioblastoma with unmethylated MGMT promoter: an international randomized phase 3 trial. *Neuro-Oncology*. 2022:noac099.
38. Gato-Cañás M, Zuazo M, Arasanz H, et al. PDL1 signals through conserved sequence motifs to overcome interferon-mediated cytotoxicity. *Cell Rep*. 2017;20(8):1818–1829.
39. Wainwright DA, Chang AL, Dey M, et al. Durable therapeutic efficacy utilizing combinatorial blockade against IDO, CTLA-4, and PD-L1 in mice with brain tumors. *Clin Cancer Res*. 2014;20(20):5290–5301.
40. Reardon DA, Gokhale PC, Klein SR, et al. Glioblastoma eradication following immune checkpoint blockade in an orthotopic, immunocompetent model. *Cancer Immunol Res*. 2016;4(2):124–135.
41. Liu CJ, Schaettler M, Blaha DT, et al. Treatment of an aggressive orthotopic murine glioblastoma model with combination checkpoint blockade and a multivalent neoantigen vaccine. *Neuro-Oncology*. 2020;22(9):1276–1288.
42. Saha D, Martuza RL, Rabkin SD. Macrophage polarization contributes to glioblastoma eradication by combination immunovirotherapy and immune checkpoint blockade. *Cancer Cell*. 2017;32(2):253–267.e5.
43. Lin H, Wei S, Hurt EM, et al. Host expression of PD-L1 determines efficacy of PD-L1 pathway blockade-mediated tumor regression. *J Clin Invest*. 2018;128(2):805–815.
44. Tang H, Liang Y, Anders RA, et al. PD-L1 on host cells is essential for PD-L1 blockade-mediated tumor regression. *J Clin Invest*. 2018;128(2):580–588.
45. Lamano JB, Lamano JB, Li YD, et al. Glioblastoma-derived IL6 induces immunosuppressive peripheral myeloid cell PD-L1 and promotes tumor growth. *Clin Cancer Res*. 2019;25(12):3643–3657.
46. Nayak L, Standifer N, Dietrich J, et al. Circulating immune cell and outcome analysis from the phase II Study of PD-L1 blockade with durvalumab for newly diagnosed and recurrent glioblastoma. *Clin Cancer Res*. 2022;28(12):2567–2578.
47. Jacques FH, Nicholas G, Lorimer IAJ, et al. Avelumab in newly diagnosed glioblastoma. *Neurooncol Adv*. 2021;3(1):vdab118.
48. Kowanetz M, Zou W, Gettinger SN, et al. Differential regulation of PD-L1 expression by immune and tumor cells in NSCLC and the response to treatment with atezolizumab (anti-PD-L1). *Proc Natl Acad Sci USA*. 2018;115(43):E10119–E10126.
49. Singh K, Batich KA, Wen PY, et al. Designing clinical trials for combination immunotherapy: a framework for glioblastoma. *Clin Cancer Res*. 2022;28(4):585–593.
50. Cloughesy TF, Mochizuki AY, Orpilla JR, et al. Neoadjuvant anti-PD-1 immunotherapy promotes a survival benefit with intratumoral and systemic immune responses in recurrent glioblastoma. *Nat Med*. 2019;25(3):477–486.